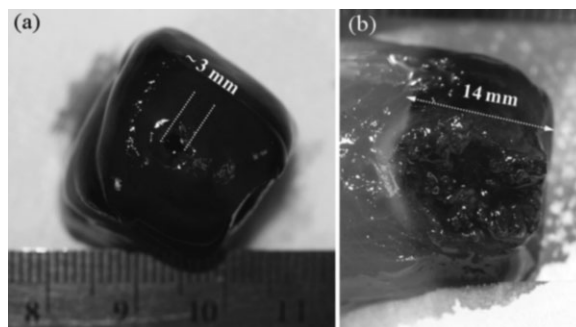


# An Electrical Thrombectomy Device Using Plasma Created Chemistry in a Saline Environment to Dissolve Vascular Clots

Jae-Chul Jung, Il Gyo Koo,\* Myeong Yeol Choi, Zengqi Yu, Myung-Soo Kim, George J. Collins\*

An electrical thrombectomy device, using liquid plasma generated radicals for removing intravascular blood clots, causing either the chronic total occlusion clots or DVT clots, was demonstrated. We employed a proxy experimental clot model of DVT with the blood filled collagen sheets. We also treated a real equine blood clot. Both clot samples were provided by the Veterinary Hospital of Colorado State University. Optical emission spectroscopy was used to examine the relative populations of the reactive chemical species generated by the liquid plasma that drives the clot dissolution during 10 min. of liquid plasma treatment at 20 W of average input power. The removal rate of the blood clots is typically up to  $2 \text{ mm}^3$  per minute and cylindrical volumes of 3 mm diameter and 14 mm long were removed. The thermal damage to contiguous tissue at the periphery of the removal volume was determined to be  $>200 \mu\text{m}$  from conventional histology analysis. We determined by FTIR spectroscopy that the collagen denaturing in liquid plasma occurs primarily via Amide III bond breakage.



## 1. Introduction

Liquid plasma originated with electric discharge machining (EDM) studies of inorganic materials, especially metals and ceramics.<sup>[1–5]</sup> Early EDM studies were often restricted to dielectric liquids with low electrical conductivity.

Based on results herein, we judge that liquid plasma in conductive saline solutions is a viable candidate for tissue processing inside the body and specifically for clot treatment

within blood vessels. Liquid plasmas in saline environment have been previously studied for electrosurgical tissue ablation,<sup>[6]</sup> as well as otolaryngology and arthroscopic procedures.<sup>[7–8]</sup> The pioneering works were reported by Slager et al.<sup>[9]</sup> in which electrical spark erosion technique for tissue processing in cardiology was proposed, and by Stalder et al.<sup>[10–13]</sup> provided basic understanding of liquid plasma using saline solutions by  $V-I$  studies, and optical studies coupled with numerical modeling of vapor layers formed in front of electrodes immersed in saline.<sup>[14–16]</sup>

Herein liquid saline solutions, with high electrical conductivity, above  $1 \text{ S} \cdot \text{m}^{-1}$ , and high (1–2 M) molar concentrations are employed as the chemical feedstock source for generating reactive chemical species to remove two types of clots. Molar concentrations of dissolved salts

J.-C. Jung, I. G. Koo, M. Y. Choi, Z. Yu, M.-S. Kim, G. J. Collins  
Department of Electrical and Computer Engineering, Colorado  
State University, Fort Collins, Colorado 80523, USA  
Fax: +1 970 491 8671; E-mail: ilgyokoo@gmail.com,  
gcollins@engr.colostate.edu

offer the possibility of high flux of radicals on the treatment surfaces, when the radicals are activated by liquid plasma conditions. Deep vein thrombosis (DVT) clots or chronic total occlusion (CTO) clots are commonly described as the formation of a thrombus, in the deep leg vein.<sup>[17]</sup> DVT's occurrence can cause an emergency such as a cardiac infarction and a lethal pulmonary embolism or for an organ can lead to necrosis or significant damage due to reduced blood flow.<sup>[18]</sup> General clinical methods presently practiced are pharmacologically or mechanically based via the injection of anticoagulants or insertion of physical devices like PTA balloons, aspiration catheters, and peripheral vascular stents to both capture and remove clots. In some cases laser ablation is employed for patients who have chronic DVTs. However, all conventional treatments have persistent limiting issues such as: lack of complete dissolution of clots with residual small particles, minimal accessible venous size with existing technology, especially for neurovascular applications, inadvertent secondary intravascular inflammation induction, damage to vessel walls and residual pieces of remaining clots leaving the clot removal zone.<sup>[19–22]</sup>

Our group recently demonstrated that liquid saline plasma could inactivate and remove undesired bacterial biofilms located on the tissue surface of human skin, without creating contiguous tissue damage to the underlying layers of dermis.<sup>[23]</sup> The main objective of the work described herein is to extend these studies to explore the feasibility of an electrical thrombectomy device, applicable to the chemically selective removal of both chronic and normal clots within blood vessels, with minimal collateral damage to vessel walls. We create electrical liquid plasma conditions, via electrode design and power delivery electronics choices, as well as various salt concentrations, which together provide unique sets of reactive radicals. The radicals are present only when electrical energy is present and are located near to the electrodes, creating reactive radicals that drive clot removal via dissolution. In addition the radicals are limited spatially by the choice of electrode geometries, herein a point electrode is described but other geometric configurations are possible. Movement of radicals downstream from the generation is minimal due to radical quenching in liquid environments where electrical discharge does not occur.

A proxy model of chronic total occlusions, using a blood filled collagen sheets, was employed. For simple clot removal fresh equine blood clots were employed. We demonstrate that both the proxy and isolated intravascular blockages can be removed at high rates ( $2 \text{ mm}^3 \cdot \text{min}^{-1}$ ) and at low temperature ( $35^\circ\text{C}$ ) by liquid plasma with minimal ( $\leq 200 \mu\text{m}$ ) thermal damage to surrounding tissue as determined via standard histology analysis. Moreover we demonstrate that collagen denaturing and removal via dissolution is driven by liquid plasma generated radicals

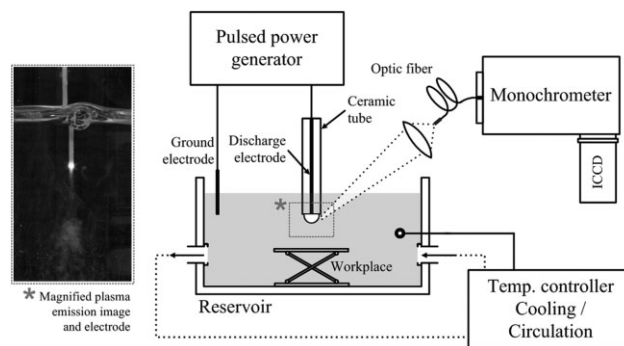


**Figure 1.** A schematic diagram of the pin electrode saline plasma system configuration for the feasibility studies of intravascular blood clot removal.

breaking Amide III bonds as evidenced by optical emission spectroscopic analysis and FTIR studies with our given experimental conditions.

## 2. Experimental Section

A schematic diagram of the liquid plasma and its application to the intravascular blood clot removal is shown in Figure 1. A pulse generator (Advanced Energy, PINACLE Plus), with arc control, gives a short pulse electrical excitation to the saline plasma, thereby minimizing the formation of vapor bubbles. 20 W of average input power was applied to the electrode with a 10% pulse width and a 20 kHz repetition frequency was employed. The voltage waveform is a rectangular pulse with a negative polarity so that negative voltage with  $5 \mu\text{s}$  of pulse width is applied to the electrode tip, periodically. A return electrode grounded was located at the periphery of the reservoir as shown in Figure 1, in which the electrode is a circular carbon rod with 3 mm diameter that was placed in 1 cm deep in the saline solution and at 8 cm distance from the main discharge electrode. The peak discharge current was 0.6–0.7 A and the peak voltage pulse magnitude was 450 V. The voltage and current delivered from the tip of the electrode to the liquid solution were measured by the high voltage probe (LeCroy, PPE 6 kV) and current probe using transformer coil (Bergoz, CT-B2.5), respectively, to determine power delivery. The average input power delivered to the saline was calculated from the multiplication of the voltage and current waveform recorded by probes during one cycle of the frequency.

A unipolar electrode of tungsten wire with 0.2 mm diameter covered by an alumina tube was employed in this study, but bipolar electrode designs, not presented here, allow for better tailoring of the spatial region of radical generation. A circulation cooling system (NESLAB, RTE-111) was used to maintain the bulk saline temperature at room temperature at all electrical energy levels employed in our study to maintain a constant ambient. The temperature of saline solution, near the electrode tip was held below  $35^\circ\text{C}$  using a circulation and cooling system, as shown in Figure 1. The generated plasma was delivered to the surface of blood clot sample by varying the distance between the electrode and the tissue sample surface. This distance was controlled by using a three-axis translation stage, and was typically several mm.

The optical emission spectrum from the saline was measured by an optical system comprised of a monochromator (Princeton Instrument, SpectroPro<sup>®</sup>-2750), a collimator lens, and an optic fiber (QFP-455-3) as shown in Figure 1. Emission spectra give qualitative information of the locally generated plasma chemistry near the electrode tip. The rotational temperature near the electrode tip at given input powers were obtained by the comparison between the measured spectra of the excited OH band and the numerical simulation results from the LIFBASE,<sup>[24]</sup> which is a program for the simulation of electronic transition behavior and transition probability calculation on the diatomic molecules like OH. The corresponding rotational temperatures were obtained from the hydroxyl OH molecular band ( $A^2\Sigma^+, v=0 \rightarrow X^2\Pi, v'=0, 306\text{--}310\text{ nm}$ ).<sup>[25–26]</sup> The rotational temperature in the thin vapor layer surrounding the electrode tip located in saline solution was measured to be around 2700 K at 20 W of average power by this spectroscopic analysis. The high resolution of spectra measured at the period of the hydroxyl band using  $3600\text{ g}\cdot\text{mm}^{-1}$  mirror. The vapor layer temperature was found to have a linear increasing dependency with electrical input power from 2350°K at 5 W of input power to 3000°K at 30 W, respectively.

The chemical functional groups of collagen before and after the liquid plasma irradiation were characterized in the wavenumber region from 2000 to 800  $\text{cm}^{-1}$  using Nicolet 6700 attenuated total reflection Fourier transform infrared (ATR-FTIR) spectroscopy system. IR spectra were collected by an average over 25 scans with a resolution of 2  $\text{cm}^{-1}$  in absorbance mode.

The extent of thermal effects on the periphery of the clot removal volumes materials is observed by use of the polarizing microscopy and histology. Birefringence arises from the linear and circular anisotropy of proteins such as collagen. So, when the temperature of the tissue is raised above a melting threshold, the collagen molecules unfold and the rod like triple-helix structure is lost, resulting in a loss of tissue birefringence.<sup>[27–29]</sup> We employed this birefringence based thermal damage measurement technique on stacked collagen sheets in our proxy model described below to track thermal damage.

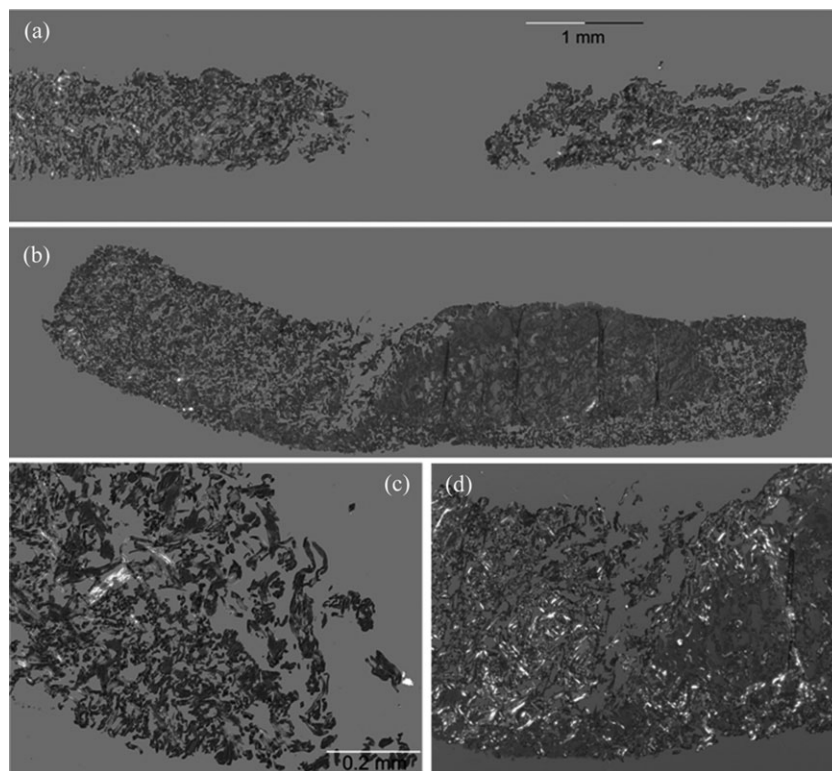
### 3. Results and Discussion

Figure 1 shows a schematic diagram of the liquid plasma system for blood clot removal of the two clot types described previously. The plasma discharge emanates from a pin electrode surrounded by saline solution. A proxy model of a chronic total occlusion, consisting of 8-tandem collagen (Medline Industries Int., PURACOL PULS) sheets soaked in blood, was placed in the saline solution and the plasma was initiated. Figure 2 shows a



**Figure 2.** Each collagen sheet is soaked with soft horse blood and a stack of eight such sheets was used as a proxy model of a chronic total occlusion blood clot. Point source electrode driven saline plasma radicals totally etched through all eight layers, removing a 2  $\text{mm}^3$  volume per minute.

multi-sheet collagen proxy, after being treated under liquid plasma conditions described above for duration of 10 min for a total energy dose of 1.2 kJ. Liquid plasma treatment removes the collagens in the region near to the point electrode only, and creates a cylindrical hole as shown in Figures 2 and 6.



**Figure 3.** 20 W of average power was applied for 10 min with minimal thermal damage ( $\leq 200\ \mu\text{m}$ ) at the periphery of the volume of cylindrical clot removal. Histological analysis employed the Pico-sirius Red dye to enhance observation of tissue birefringence changes using conventional polarizing microscopy.

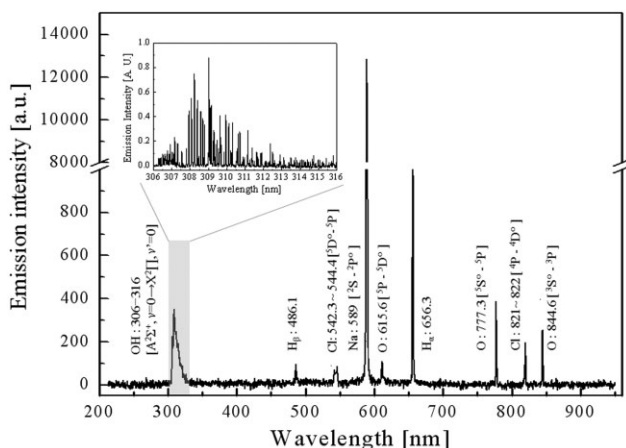
In Figure 2 eight tandem collagen sheets each soaked with the soft horse-blood were used as a proxy chronic total occlusion clot model. The saline plasma was directed on the proxy for various saline plasma exposure times. After saline plasma irradiation each stacked collagen sheet was stained with the Picro-sirius Red.<sup>[30]</sup> Figure 3a and b show histological cross-sectional images of contiguous collagen layers, respectively, where volume collagen removal occurred in the central portion, and little damage occurred in the periphery beyond 0.2 mm as shown in Figure 3 histology.

Figure 3a displays a bright yellow or orange color of the large collagen fiber. Thermal damage and structural change by protein denaturing in adjacent periphery tissue is limited to a zone smaller than 0.2 mm as shown in Figure 3c, which focuses on the magnified image of the edge region of Figure 3a where inadvertent periphery damage is desired to be minimal. Figure 3b illustrates the bottom, or the eighth layer, of the stacked collagen proxy, just before the liquid plasma removes a circular hole through it. This illustrates undamaged collagen structures in the periphery. The magnified image, in Figure 3d, illustrates that disjunction of the local collagen structure is taking place by liquid plasma irradiation without denaturing of adjacent protein. Figure 3d shows the edge region of Figure 3b with the same minimal damage apparent. The larger secondary damage at the top collagen layer observed as it arises from the increased total irradiation or treatment time required to treat all eight layers of collagen in our proxy model. In summary, the peripheral damage from the liquid plasma on the edge of collagen sheet removal is measured to be <0.2 mm by histological studies.

The dominant spectral lines emitted by the saline plasma are shown in Figure 4. We observed reactive radicals such

as: hydroxyl, hydrogen, chloride, and oxygen species occurs as well as large neutral sodium atom line intensity.<sup>[17–23,30]</sup> We then subsequently confirmed that the collagen denaturing stems from the chemical reaction with radical species rather than pure thermal conditions as follows. As the gas phase plasma ignites within a thin bubble contacted to the electrode surface, an intense sodium atom line (589 nm) is emitted, which is due to the abundant excited sodium atoms created, because the threshold excitation energy of the sodium atom by an electron impact is much lower as 2.1 eV than other atomic or molecular state. In contrast, other optical emissions from the excited hydroxyl, hydrogen atom, and oxygen atoms originate in the vapor phase by electron impact dissociation from the water molecules and secondary reactions. Conversion of dissolved negative chlorine ions in saline to excited chlorine atoms by electron excitation, occurs as evidenced by chlorine I spectrum.<sup>[31]</sup>

In Figure 5, we compare FT-IR spectrum from the untreated collagen sheet control versus the saline plasma treated collagen. The byproducts of the reactions were collected from the liquid plasma reactor for collagen samples exposed to a saline solution for 1 min at 20 W. Using FT-IR spectrometer for absorption studies, we observed major functional groups of the collagen sheet before and after saline plasma irradiation. Biggest changes occurred with the following well-established molecular species: Amide II ( $1543\text{ cm}^{-1}$ ),  $\text{CH}_2$  bending mode ( $1459\text{ cm}^{-1}$ ),  $\text{COO}^-$  stretching mode ( $1400\text{ cm}^{-1}$ ), and Amide III ( $1239\text{ cm}^{-1}$ ).<sup>[32]</sup> The reduction in intensity of the Amide III band prominently observed in the FT-IR spectra indicates a chemical driven protein denaturation occurs when exposed to the saline plasma. An *ex vivo* blood clot removal by liquid plasma irradiation employing a horse



**Figure 4.** The dominant spectral lines emitted by the saline plasma. Note the presence of two Cl emissions under our experimental saline plasma conditions, indicating the conversion of the negative Cl ion to neutral chlorine in our conditions.

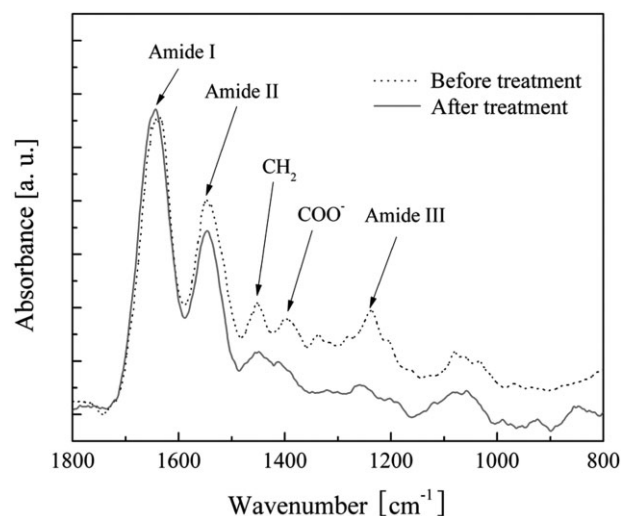


**Figure 5.** FT-IR spectra analysis for the collagen sheets treated in saline plasma as compared to untreated samples, in the wavelength region from 1800 to 800  $\text{cm}^{-1}$ .

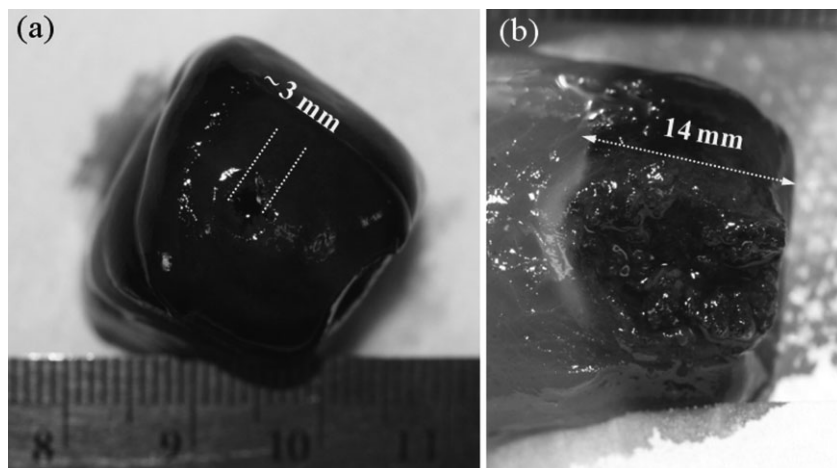


**Figure 6.** Successful removal of an ex vivo equine blood-clot by the pin electrode configuration after 7 min treatment by liquid plasma irradiation in a saline environment.

Keywords: blood clot; electric discharge; liquid plasma; saline solution; thrombectomy

blood clot was demonstrated. After 7 min of saline plasma irradiation at 20 W of average input power, a 3 mm wide and 14 mm long cylindrical hole was created by liquid plasma as shown in Figure 6a and b shows the cross-sectional picture of the blood clot sample after the liquid plasma treatment.

#### 4. Conclusion

The feasibility of employing an electrical thrombectomy device for removing blood clots by chemical dissolution, using liquid plasma in saline solution, was explored. We achieved successful electrical intravascular excision, 3 mm wide by 14 mm long, on our proxy model of a chronic total occlusion and similar results with simple clots. It was confirmed by histological analysis that we created minimum ( $\leq 200 \mu\text{m}$ ) contiguous tissue damage. Chemically driven collagen denaturing is verified by FT-IR spectroscopic analysis, and predominant reactive chemical species were identified by the emission spectroscopy studies.

**Acknowledgements:** This work was supported by the National Research Foundation of Korea and by the Bioscience Discovery Evaluation Grant Program of the Colorado State Government (Office of Economic Development and International Trade; BGEGP-10BGF-25) as well as by NSF. The Korean Grant is funded by the Korean Government (Ministry of Education, Science and Technology; NRF-2010-357-D00104).

Received: July 12, 2011; Revised: December 18, 2011; Accepted: January 6, 2012; DOI: 10.1002/ppap.201100142

- [1] J. L. Maksiejewski, J. H. Calderwood, *Nature* **1968**, *220*, 905.
- [2] P. Barmann, S. Kroll, A. Sunesson, *J. Phys. D: Appl. Phys.* **1997**, *30*, 856.
- [3] P. Sunka, V. Babicky, M. Clupek, P. Lukes, M. Simek, J. Schmidt, M. Cernak, *Plasma Sources Sci. Technol.* **1999**, *8*, 258.
- [4] P. K. Watson, W. G. Chadband, W. Y. Mak, *IEEE Trans. Electrical Insulation* **1985**, *EI-20*, 275.
- [5] M. L. Jeswani, *Wear* **1981**, *72*, 81.
- [6] J. Woloszko, C. Gilbride, *Proc. Int. Soc. Opt. Phot. (SPIE)* **2000**, *3907*, 306.
- [7] J. D. Polousky, T. P. Hedman, C. T. Vangesness, Jr., *Arthroscopy* **2000**, *16*, 813.
- [8] K. R. Stalder, J. Woloszko, I. G. Brown, C. D. Smith, *Appl. Phys. Lett.* **2001**, *79*, 4503.
- [9] C. J. Slager, C. E. Essed, J. C. H. Schuurbers, N. Bom, P. W. Serruys, G. T. Meester, *J. Am. Coll. Cardiol.* **1985**, *5*, 1382.
- [10] J. Woloszko, K. R. Stalder, I. G. Brown, *IEEE Trans. Plasma Sci.* **2002**, *30*, 1376.
- [11] J. Woloszko, M. Kwende, K. R. Stalder, *Proc. Int. Soc. Opt. Phot. (SPIE)* **2003**, *341*, 4949.
- [12] K. R. Stalder, G. Nersisyan, W. G. Granham, *J. Phys. D: Appl. Phys.* **2006**, *39*, 3457.
- [13] K. R. Stalder, J. Woloszko, *Contrib. Plasma Phys. Lett.* **2007**, *47*, 64.
- [14] K. R. Stalder, D. F. McMillen, J. Woloszko, *J. Phys. D: Appl. Phys.* **2005**, *8*, 1728.
- [15] L. Schaper, W. G. Graham, K. R. Stalder, *Plasma Source Sci. Technol.* **2011**, *20*, 034003.
- [16] L. Schaper, W. G. Graham, K. R. Stalder, *Plasma Source Sci. Technol.* **2011**, *20*, 034004.
- [17] J. J. Cronan, *Radiology* **1993**, *186*, 619.
- [18] T. M. Chapman, K. L. Goa, *Drugs* **2003**, *63*, 2357.
- [19] L. T. Cotton, V. C. Roberts, *Surgery* **1977**, *81*, 228.
- [20] P. Mismetti, S. Laporte, J.-Y. Carmon, A. Buchmuller, H. Decousus, *Br. J. Surg.* **2001**, *88*, 913.
- [21] W. L. Monskey, S. Finisis, D. D. Cicco, J. M. Brock, J. Kucharczyk, R. E. Latchaw, *Cardiovasc. Intervent Radiol.* **2011**, *34*, 383.
- [22] D. Scrvelis, P. S. Wells, *CMAJ* **2006**, *175*, 1087.
- [23] P. Y. Kim, Y. S. Kim, I. G. Koo, J. C. Jung, G. J. Kim, M. Y. Choi, Z. Yu, G. J. Collins, *PLoS ONE* **2011**, *6*, e241104.
- [24] J. Luque, D. R. Crosley, LIFBASE: Database and spectral simulation (version 2.0), SRI Int.
- [25] I. G. Koo, J. H. Cho, W. M. Lee, *Plasma Process. Polym.* **2008**, *5*, 161.
- [26] C. O. Laux, T. G. Spence, C. H. Kruger, R. N. Zare, *Plasma Source Sci. Technol.* **2004**, *12*, 125.
- [27] C. Cohen, *J. Biophys. Biochem. Cytol.* **1955**, *1*, 203.
- [28] K. Schoenenberger, B. W. Colston, Jr., D. J. Maitland, L. B. Da Silva, M. J. Everett, *J. Appl. Opt.* **1998**, *37*, 6026.
- [29] S. Thomsen, J. A. Pearce, W. F. Cheong, *IEEE Trans. Biomed. Eng.* **1989**, *36*, 1174.
- [30] J. D. Holcomb, K. J. Kent, D. E. Rousso, *Arch. Facial Plast. Surg.* **2009**, *11*, 184.
- [31] G. R. Harrison, "Wavelength Tables," The M.I.T. Press, Massachusetts **1939**.
- [32] E. O. Faolain, M. B. Hunter, J. M. Byrne, P. Kelehan, M. McNamar, H. J. Byrne, F. M. Lyung, *Vib. Spect.* **2005**, *38*, 121.